symmetry

MDPI

Article

Experimental Review of $\Lambda\bar{\Lambda}$ Production

Xiaorong Zhou [1,2,*], Liang Yan [3,*], Rinaldo Baldini Ferroli [4,*] and Guangshun Huang [1,2,*]

1 Department of Modern Physics, University of Science and Technology of China, Hefei 230026, China
2 State Key Laboratory of Particle Detection and Electronics, Hefei 230026, China
3 Key Laboratory of Nuclear Physics and Ion-beam Application (MOE) and Institute of Modern Physics, Fudan University, Shanghai 200443, China
4 INFN Laboratori Nazionali di Frascati, I-00044 Frascati, Italy
* Correspondence: zxrong@ustc.edu.cn (X.Z.); yanl@fudan.edu.cn (L.Y.); Rinaldo.Baldini@lnf.infn.it (R.B.F.); hgs@ustc.edu.cn (G.H.)

Abstract: Exclusive hyperon-antihyperon production provides a unique insight for understanding of the intrinsic dynamics when strangeness is involved. In this paper, we review the results of $\Lambda\bar{\Lambda}$ production via different reactions from various experiments, e.g., via $\bar{p}p$ annihilation from the LEAR experiment PS185, via electron-positron annihilation using the energy scan method at the CLEO-c and BESIII experiments and the initial-state-radiation approach utilized at the BaBar experiment. The production cross section of $\Lambda\bar{\Lambda}$ near the threshold is sensitive to QCD based prediction. Experimental high precision data for $\bar{p}p \to \bar{\Lambda}\Lambda$ close to the threshold region is obtained. The cross section of $e^+e^- \to \Lambda\bar{\Lambda}$ is measured from its production threshold to high energy. A non-zero cross section for $e^+e^- \to \Lambda\bar{\Lambda}$ near threshold is observed at BaBar and BESIII, which is in disagreement with the pQCD prediction. However, more precise data is needed to confirm this observation. Future experiments, utilizing $\bar{p}p$ reaction such as PANDA experiment or electron-positron annihilation such as the BESIII and BelleII experiments, are needed to extend the experimental data and to understand the $\Lambda\bar{\Lambda}$ production.

Keywords: $\Lambda\bar{\Lambda}$ production; threshold; cross section

Citation: Zhou, X.; Yan, L.; Ferroli, R.B.; Huang G. Experimental Review of $\Lambda\bar{\Lambda}$ Production. *Symmetry* **2022**, *14*, 144. https://doi.org/10.3390/sym14010144

Academic Editor: Ignatios Antoniadis

Received: 30 November 2021
Accepted: 1 January 2022
Published: 12 January 2022

1. Introduction

The Λ hyperon, as the first baryon discovered containing the strange quark [1,2], is of great importance in the elaboration of the Standard Model (SM). While the SM of particle physics and the perturbative Quantum Chromodynamics (pQCD) can successfully describe the experimental results at high energies, the study of the strong interaction at low energies confronts great challenges since perturbative methods is not applicable. Among these, exclusive $\Lambda\bar{\Lambda}$ production, whose four-momenta transfer is of the same magnitude as the asymptotic scale parameter Λ_{QCD}, allows us to study the internal dynamics with strangeness and can be used to probe various QCD-motivated models.

The $\Lambda\bar{\Lambda}$ production can be studied in reactions with strangeness exchange like the process $\bar{p}p \to \bar{\Lambda}\Lambda$ with an intermediate strange meson, e.g., K or K^*. Since the intermediate mesons are relatively heavy, the production of hyperons is a short-ranged process and thus can't be described with perturbative methods. Usually, $\bar{p}p \to \bar{\Lambda}\Lambda$ is analyzed on the level of quark and gluon degrees of freedom [3], instead of using meson-exchange model. Therefore, the reaction can be interpreted as an annihilation of a pair of two non-strange quarks and the creation of a pair of strange quarks, which is called vacuum pair creation (VPC). A different interpretation uses gluon intermediate states associated with scalar diquarks and is denoted as one-gluon-exchange (OGE). The OGE model relies on the perturbative gluon exchange in the lowest order, thus is typically S-wave. It predicts the cross section of $\bar{p}p \to \bar{\Lambda}\Lambda$ near threshold follows a $(s - s_0)^{1/2}$ energy dependence, where s is the center-of-mass (c.m.) energy square and $s_0 = 4m_\Lambda^2$ with m_Λ the mass of Λ from PDG [4]. The VPC model favors $^3P_0$ that the cross section follows a $(s - s_0)^{3/2}$ energy dependence. Experimentally, with

the low-energy anti-proton at LEAR, a systematic study of the production mechanism for hyperon-antihyperon pairs in $\bar{p}p$ annihilation is performed.

The $\Lambda\bar{\Lambda}$ production can also be studied from electron-positron annihilation process, $e^+e^- \to \Lambda\bar{\Lambda}$. Under one-photon-exchange (OPE) approximation, the differential Born cross section for the process $e^+e^- \to \Lambda\bar{\Lambda}$ can be expressed in terms of electric and magnetic FFs, G_E and $G_M|$ [5], which is applicable for any spin 1/2 baryon.

$$\frac{d\sigma^B(s)}{d\Omega} = \frac{\alpha^2\beta C}{4s}\left[|G_M(s)|^2(1+\cos^2\theta) + \frac{1}{\tau}|G_E(s)|^2\sin^2\theta\right], \quad (1)$$

In above equation, $\alpha \approx \frac{1}{137}$ is the electromagnetic fine-structure constant, $\beta = \sqrt{1-4m_\Lambda^2/s}$ is the phase-space factor, $\tau = s/4m_\Lambda^2$ and θ is the polar angle of final baryon in its c.m. production angle. The Coulomb correction factor C [6,7], which accounts for the electromagnetic interaction of final states, is $y/(1-e^{-y})$ with $y = \pi\alpha(1+\beta^2)/\beta$ for a charged baryon pair and 1 for a neutral baryon pair. Since at threshold, $G_E = G_M = G$ by definition, the production cross section of $e^+e^- \to \Lambda\bar{\Lambda}$ is proportional to the β near threshold, that vanishes at threshold due to $\beta = 0$ and raises with finite β above threshold. There are many experimental measurements of $e^+e^- \to \Lambda\bar{\Lambda}$ and the corresponding form factors exist. Two kinds of experimental approaches are available, the energy scan method, where measurements of the cross sections are performed by taking data at fixed c.m. energies, taking advantage of the finite beam energy resolution of e^+e^- colliders; and the initial-state-radiative (ISR) approach, where the next higher order of the examined process is used for the measurement. Currently, the energy scan method is performed at the experiments with operating c.m. energy in tau-charm energy region which covers the threshold of various hyperon pair production, and the ISR approach is performed at the B factories.

2. Experiments and Datasets

Various experiments have been performed to study the exclusive production of $\Lambda\bar{\Lambda}$. The PS185 experiment measured the strangeness exchange reaction $\bar{p}p \to \bar{\Lambda}\Lambda$ [8–10]. The DM2, CLEO-c and BESIII experiments measured the $\Lambda\bar{\Lambda}$ production from electron-positron annihilation $e^+e^- \to \Lambda\bar{\Lambda}$ by means of the energy scan method [11–14] and BaBar measured $e^+e^- \to \Lambda\bar{\Lambda}$ with the ISR approach [15].

2.1. The PS185 at LEAR

The CERN Low Energy Antiproton Ring (LEAR) project was launched in 1982 [16] which provided a high-quality antiproton beams with momentum from 100 MeV/c to 2 GeV/c. There have been many experiments been performed at LEAR, such as the measurement of the annihilation and elastic cross sections of $\bar{p}p$, the $\bar{p}p$ charge-exchange reaction $\bar{p}p \to \bar{n}n$ and the strangeness-exchange reaction $\bar{p}p \to \bar{Y}Y$ with Y denotes hyperon. The aim of the PS185 experiment operating at LEAR is to study how the strange quarks are produced, where one of the most precise results at PS185 is the study of $\bar{p}p \to \bar{\Lambda}\Lambda$ [8–10].

The target of the PS185 detector consists four 2.5 mm thick cylinder material made with CH_2 with diameter 2.5 mm. The detection system consists a sets of multiwire proportional chambers and drift chambers for the reconstruction of charged tracks, a scintillator hodoscope for the trigger, and an additional drift chambers in a magnetic field of $B = 0.09$ T. The kinematic region of $\bar{p}p \to \bar{Y}Y$ processes performed at PS185 experiment is from threshold to nearly 200 MeV above. The $\bar{p}p \to \bar{\Lambda}\Lambda$ process is identified by reconstructing two decay vertices of $\Lambda \to p\pi^-$ and $\bar{\Lambda} \to \bar{p}\pi^+$ and performing a full kinematic fit under the assumption of $\bar{p}p \to \bar{\Lambda}\Lambda \to \bar{p}\pi^+p\pi^-$. Finally, a χ^2 requirement from kinematic fit is applied for a good signal event. Two kinds of background sources contaminated in the signal are studied, one is the $\Lambda\bar{\Lambda}$ events produced on the carbon nuclei of the target cell CH_2, which is estimated by counting such events produced in a pure carbon target, the other is the non-Λ events which can be estimated by the taking data that below threshold.

2.2. The DM2 at DCI

The DM2 experiment [17] operating at DCI is a large solid angle spectrometer with c.m. energy range from 1.2 to 3.7 GeV of e^+e^- collision. A 0.5 T field is produced by the magnetic solenoid. Two proportional and drift chambers provide measurement of charged track with a momentum resolution of 3.5% at 1 GeV/c. A system of scintillation counters gives a time-of-flight information with an intrinsic resolution of 330 ps. The photon detector is designed to measure the photon with a precision of 1° and a good detection efficiency for low energy photons (50 MeV). Outside the photon detector, there are two vertical concrete absorbers and two horizontal iron absorbers, which serve as a muon identifier. The coverages for charged particles and photons are 87% and 82% of 4π, respectively.

With an integrated luminosity of 161 nb^{-1}, the $e^+e^- \to \Lambda\bar{\Lambda}$ process at $\sqrt{s} = 2.386$ GeV has been measured at DM2 [11]. The Λ pairs are reconstructed from four charged tracks in the event with a net charge of zero, and three tracks with ± 1 charge. The four track events are required to have a missing momentum less than 0.15 GeV/c and a squared missing mass in the $p\bar{p}\pi^+\pi^-$ hypothesis within (0, 0.01) GeV$^2/c^4$. Finally, four $\Lambda\bar{\Lambda}$ events well separated from the background are selected from the four track events. The three track events are required to have one proton and one pion mass within the region of (1.08, 1.22) GeV/c^2 range. Further requirements are applied on the missing momentum and time-of-flight. After selection, no $\Lambda\bar{\Lambda}$ signal is observed in these three track events.

2.3. The BABAR at PEP-II

The PEP-II B-factory is an asymmetric e^+e^- collider that operates with a luminosity of 3×10^{33} cm^{-2} s^{-1} and above, at a c.m. energy of 10.58 GeV, the mass of the $\Upsilon(4S)$ resonance. At PEP-II, the electron beam of 9.0 GeV colliders with the positron beam of 3.1 GeV. The BaBar experiment [18] has collected an integrated luminosity of 424 fb^{-1} at $\sqrt{s} = 10.58$ GeV. At Babar, the charged particle is detected in a multi-layer silicon vertex tracker surrounded by a cylindrical wire drift chamber with a transverse momentum resolution of 0.47% at 1 GeV/c, operating in a 1.5 T magnetic field. Identification of charged particle is provided by the dE/dx ionization and an internal reflecting Ring Imaging Cherenkov Detector (DIRC). The DIRC provides a K/π separation of 4.2σ with momentum up to 3.0 GeV/c. Electromagnetic showers from electrons and photons with energy range from 20 MeV to 4 GeV are detected in an array of CsI crystals with an energy resolution of 3% at 1 GeV. Muons and other neutral hadrons are identified in the solenoid's instrumented flux return, which consists of iron plates interleaved with resistive plate chambers.

A data sample corresponding to an integrated luminosity of 230 fb^{-1} is used to measure the cross section of $e^+e^- \to \Lambda\bar{\Lambda}$ by studying the ISR process, $e^+e^- \to \Lambda\bar{\Lambda}\gamma_{ISR}$ [15]. The photon must have an energy larger than 3 GeV in the c.m. frame. At least one Λ and one $\bar{\Lambda}$ are required where the $\Lambda/\bar{\Lambda}$ is selected from two oppositely-charged tracks assigned to the proton and pion mass hypotheses with a total invariant mass within the range of (1.104, 1.128) GeV/c^2. A kinematic fit is applied under the hypothese of $\gamma\Lambda\bar{\Lambda}$ with the photon energy as a free parameter. In total, 387 events are selected with requirements from above, wherein 221 selected events have an invariant mass below 3 GeV/c and others are mostly signals from the processes $J/\psi \to \Lambda\bar{\Lambda}$ and $\psi(2S) \to \Lambda\bar{\Lambda}$. After background subtraction, the number of signal events below 3 GeV/c^2 is about 160.

2.4. The CLEO-c at CESR

The CLEO-c [19] is the experiment operating at the CESR storage ring that taking data in the c.m. energy range of 3 to 5 GeV. The tracking system of CLEO-c detector consists a six-layer inner drift chamber with wires at small stereo angles, and a 47-layer central drift chamber, providing a momentum resolution of approximately 0.6% at 1 GeV/c in a 1 T magnetic field. A Ring Imaging CHerenkov (RICH) detector is used to identify particles combined with the dE/dx information from the drift chamber. The RICH provides a kaon identification efficiency of over 90% with a fake rate from pion to be 1% with the momentum up to 1.5 GeV/c. The electromagnetic calorimeter consisting of 7800 CsI (Tl)

crystals is used to detect photons or electrons with an energy resolution of 2.5% at 1 GeV. The solid angle coverage for charged and neutral particles in the CLEO-c detector is 93% of 4π.

Data samples with an integrated luminosity of 805 pb^{-1} at $\sqrt{s} = 3.77$ GeV, and 586 pb^{-1} at $\sqrt{s} = 4.17$ GeV, are used to measure the form factors of Λ with the process $e^+e^- \to \Lambda\bar{\Lambda}$ [12]. The yields of strong interaction process, $\psi(3770) \to gluons \to \Lambda\bar{\Lambda}$, are estimated by assuming the ratio of hadronic and leptonic decays of $\psi(3770)$ is the same as that of $\psi(3686)$. It is found that contributions of such strong decays are negligible. Thus the observed events at $\sqrt{s} = 3.77$ GeV mostly arise from the one-photon process $e^+e^- \to \gamma^* \to B\bar{B}$. The Λ is reconstructed by fitting two oppositely charged tracks into a common vertex, where the decay vertex must be away from the interaction point (IP) over 2 mm and the invariant mass within 5σ of the nominal mass of Λ [4]. The $\Lambda\bar{\Lambda}$ signal is selected with a total momentum of $<$50 MeV/c. Finally, a number of 105 ± 10 signal events is obtained for $e^+e^- \to \Lambda\bar{\Lambda}$.

2.5. The BESIII at BEPCII

The Beijing electron-positron collider, BEPCII, is a double ring symmetric collider running with c.m. energies from 2.0 to 4.95 GeV, with a peaking luminosity of 1×10^{33} cm^{-2} s^{-1} achieved at a beam energy of 1.89 GeV. The BESIII detector [20] is a cylindrical detector which covers 93% of the full solid angle. It consists of several sub-detectors. A small cell, helium based (60% He, 40% C_3H_8) Main Drift Chamber (MDC) in a 1 T magnetic field which provides momentum measurements of charged particles with a resolution of 0.5% at 1 GeV/c. The energy loss measurement (dE/dx) provided by the MDC has a resolution better than 6%. A Time-of-Flight (TOF) system consisting of 5-cm-thick plastic scintillators has a time resolution of 80 ps in the barrel region and 65 ps in the endcaps. An Electromagnetic Calorimeter (EMC) consisting of 6240 crystals made with CsI(Tl) is arranged in a cylindrical structure and two endcaps, which can be used to measure the energies of electrons and photons. The energy resolution of the EMC for 1 GeV electrons or photons is 2.5% in the barrel and 5% in the end caps. The position resolution of the EMC is 6 mm in the barrel and 9 mm in the end caps for 1 GeV electrons or photons. It should be noted that the EMC can also be used to identify other neutral tracks, like K_L and $\bar{n}$, but with only part of their total energies deposited. The outmost is a Muon Chamber consisting of 1000 m^2 of resistive plate chambers, which can be used to identify muons with a spatial resolution better than 2 cm.

BESIII has accumulated the world largest data samples of e^+e^- collisions in the tau-charm region. There are rich physics outputs from $\Lambda\bar{\Lambda}$ studies at BESIII [13,14,21–24]. Besides, BESIII has measured the production cross sections of various baryon pairs in the time-like region [25]. Despite the fact that there are wide physics programs at BESIII concerning the production of $\Lambda\bar{\Lambda}$ at ψ [22] resonances, and the polarization of Λ at different c.m. energies [14,23,24], we only focus on the production cross section of $e^+e^- \to \Lambda\bar{\Lambda}$ in the continuum region (that is away from the c.m. energy region of ψ resonances) in this draft, including data with an integrated luminosity of 40.5 pb^{-1} at 4 energy points from 2.2324 to 3.08 GeV [13] and data with an integrated luminosity of 20 pb^{-1} at 33 energy points from 3.51 to 4.60 GeV [14]. The study of $e^+e^- \to \Lambda\bar{\Lambda}$ at $\sqrt{s} = 2.2324$ GeV, which is only 1.5 MeV above $\Lambda\bar{\Lambda}$ threshold, is selected via two decay modes, with the final state topologies $p\bar{p}\pi^+\pi^-$ and $\bar{n}\pi^0 + X$, where X denotes inclusive decays from Λ. An indirect search for the antiproton interacted with the beam pipe is employed for $p\bar{p}\pi^+\pi^-$, which shows an enhancement in the vertex distance of secondary produced charged tracks perpendicular to the beam, V_r, around 3 cm. The soft pions from final states are selected and the momenta are required to be within (0.08, 0.11) GeV/c. A fit yields 43 ± 7 signal events for $p\bar{p}\pi^+\pi^-$ final states as shown in Figure 1a. For the final state $\bar{n}\pi^0 X$, the mono-energetic π^0 is identified after a strict selection of the antineutron with the EMC. For the latter a boosted decision tree method is employed to distinguish antineutrons from photons. After selection, 22 ± 6 signal events for $\bar{n}\pi^0 X$ are obtained from the fit as shown in Figure 1b. For

the reconstruction of $e^+e^- \to \Lambda\bar{\Lambda}$ at other c.m. energies, a method of full reconstruction of the final states $p\bar{p}\pi^+\pi^-$ is applied. There are 45 ± 7, 8 ± 3 and 13 ± 4 signal events at $\sqrt{s} = 2.40$, 2.80 and 3.08 GeV, respectively. At high c.m. energies, due to the rapid decrease of the cross section with $1/(\sqrt{s})^{10}$ [26], the number of signal events is few. It's worth to mention that with an integrated luminosity of 2.93 fb^{-1} at $\sqrt{s} = 3.773$ GeV, an amount of 261.0 ± 16.2 signal events for $e^+e^- \to \Lambda\bar{\Lambda}$ is obtained [14].

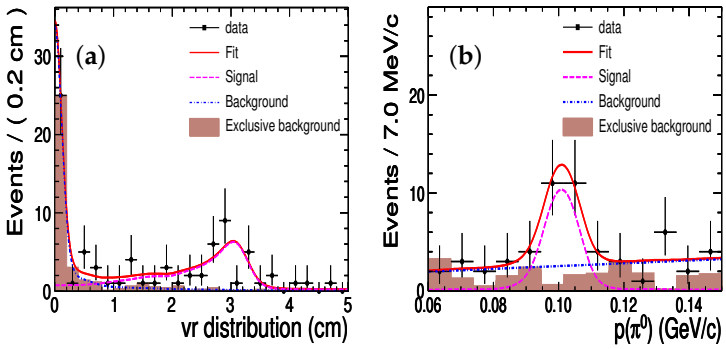

Figure 1. An illustration of the selected events at $\sqrt{s} = 2.2324$ GeV of (**a**) V_r distribution of secondary particles in $\bar{p}$ annihilating with material for $p\bar{p}\pi^+\pi^-$ final states and (**b**) the mono-momentum of π^0 for $\bar{n}\pi^0 + X$ final states. The plots are taken from Ref. [13].

3. Experimental Results

3.1. $\bar{p}p \to \bar{\Lambda}\Lambda$

The $\bar{\Lambda}\Lambda$ production at LEAR PS185 experiment is studied very close to the threshold at $s_0 = 4m_\Lambda^2$ [8–10]. The results are summarized in Figure 2a, as a function of the c.m. excess energy $\epsilon = \sqrt{s} - 2m_\Lambda$. The first measurement of $\bar{p}p \to \bar{\Lambda}\Lambda$ near threshold is carried out at sixteen points [8], with the incident momentum of antiproton to from 1432.65 MeV/c to 1446.55 MeV/c, corresponding to a excess energy from 0.85 MeV below threshold to 4.05 MeV above the $\bar{\Lambda}\Lambda$ threshold. Later on, a more precise measurement is performed in the similar excess energy region, and a structure at $\epsilon \approx 0.6$ MeV is observed [9]. An empirical fit has been performed on the cross sections with contributions from pure phase space which includes S-wave and P-wave, and a Breit-Wigner resonances [9]. The fit indicates a strong P-wave contribution near the production threshold. The most striking result is a possible structure exist from the fit, with an invariant mass of 2.231 ± 0.1 GeV and width of 0.59 ± 0.25 MeV. The experimental results as well as the fits are shown in Figure 2a. The interpretation of the resonant structure in the region around $\sqrt{s} = 2.2$ GeV includes glueballs, hybrids, multi-quark states etc. One of the explanation of this structure could be the existence of a narrow $\bar{\Lambda}\Lambda$ subthreshold state of quasi-nuclear nature [27].

This structure motivates further measurements with high accuracy for the relevant region [10]. However, results of the third experiment performed in this energy region with increased beam flux and improved detection method is in disagreement with previous results [8,9], where the apparent difference is the overall cross section that is about 15% larger than earlier experiments as shown in Figure 2a. The difference mainly comes from imperfect simulation of MC acceptance and the hadronic interaction, yielding an underestimation of 8–12% of previous results. Even so, there are still two remarkable differences of the new results from previous ones. The first is a less significant P-wave contribution compared to the previous results. The second is a smooth behavior near threshold with no evident of any resonant structure. It seems the puzzle of the threshold enhancement has been resolved. However, in a full partial wave analysis of $\bar{p}p \to \bar{\Lambda}\Lambda$ data [28], evidence of a new isospin singlet vector states with mass of 2.29 ± 0.02 GeV/c^2 and width of 0.275 ± 0.0035 GeV is provided. It is still of great interest to studying the structures or the so-called cusp effect around the thresholds in particle physics.

Figure 2b shows a view of all existing experimental results for the $\bar{p}p \to \bar{\Lambda}\Lambda$ reaction with the momentum of incident $\bar{p}$ from 1.4 to 3.7 GeV/c. The cross section shows a rapid increase from threshold to the maximum value of about 120 μb in the region of $p_{\bar{p}} > 1.7$ GeV/c. With such large cross section, huge amount of Λ hyperons can be produced from $\bar{p}p$ annihilation. Apart from the total cross section of $\bar{p}p \to \bar{\Lambda}\Lambda$, more physics programs can be studied with such reaction, including the differential cross sections, the spin polarization and spin correlations. The differential cross section of the process $\bar{p}p \to \bar{\Lambda}\Lambda$ is studied by PS185 experiment which indicates a pronounced forward peaking followed by a flat angular distribution, indicating the existence of P-wave. Results on more discussions of differential cross section as well as the polarization and spin observables of Λ can be found in review Ref. [29].

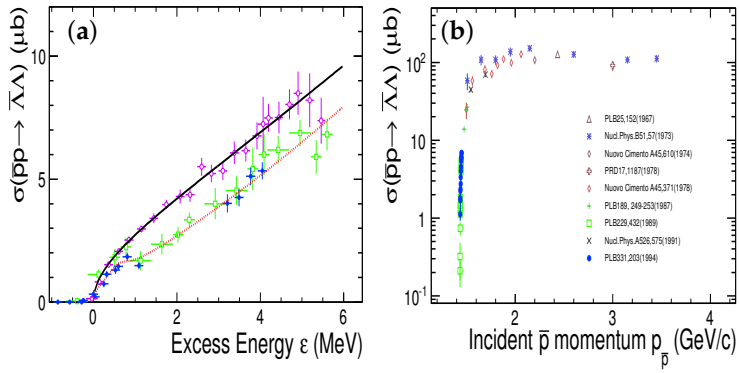

Figure 2. (**a**) Total cross section results for the $\bar{p}p \to \bar{\Lambda}\Lambda$ reaction versus excess energy near threshold. The solid circle in blue is from Ref. [8], the open square in green is from Ref. [9] and the open circle in violet is from Ref. [10]. The dotted line and solid line are two fit functions introduced in Refs. [9,10]. (**b**) Total cross section results for $\bar{p}p \to \bar{\Lambda}\Lambda$ reaction versus the incident $\bar{p}$ momentum in a wider energy range from various experiments.

3.2. $e^+e^- \to \Lambda\bar{\Lambda}$

For the measurement of $e^+e^- \to \Lambda\bar{\Lambda}$ via directly scan method, the cross section for $e^+e^- \to \Lambda\bar{\Lambda}$ is obtained through

$$\sigma^B = \frac{N_{obs}}{\mathcal{L}\varepsilon(1+\delta)\mathcal{B}'} \tag{2}$$

where N_{obs} is the number of observed events after background subtraction, $\mathcal{L}$ is the integrated e^+e^- luminosity obtained from QED processes with known cross section theoretically, ε is the efficiency depending on the detector acceptance and the event selection, $(1+\delta)$ is the radiative correction that can be obtained depending on the ISR photon energy fraction, and $\mathcal{B}$ is the product of decay branching fractions of intermediate states.

Keeping a fixed c.m. energy $\sqrt{s}$, a collection of events over a wide spectrum of energies $\sqrt{s'}$ can be obtained by the ISR photon energy fraction $x = 2E_\gamma/\sqrt{s}$, such that $s' = (1-x)s$. The cross section for $e^+e^- \to \Lambda\bar{\Lambda}$ can then be obtained from the measurement of of $e^+e^- \to \Lambda\bar{\Lambda}\gamma_{ISR}$ through

$$\sigma^B(\sqrt{s'}) = \frac{dN/d\sqrt{s'}}{\varepsilon R dL/d\sqrt{s'}} \tag{3}$$

where $dN/d\sqrt{s'}$ is the mass spectrum of $\Lambda\bar{\Lambda}$, $dL/d\sqrt{s'}$ is the effective ISR luminosity, ε is the detection efficiency as a function of $\Lambda\bar{\Lambda}$ invariant mass spectrum and R is a radiative correction factor accounting for the high order processes.

Results for cross sections of $e^+e^- \to \Lambda\bar{\Lambda}$ from both, the energy scan and the ISR methods, are presented in Figure 3. The cross sections from $\Lambda\bar{\Lambda}$ threshold to 2.5 GeV from measurements of DM2 [11], BaBar [15] and BESIII [13] are shown in Figure 3a. The DM2 experiment has observed 4 $\Lambda\bar{\Lambda}$ signals at $\sqrt{s} = 2.3864$ GeV, which yield a cross section of

100^{+65}_{-35} pb. BaBar measured the cross section of $e^+e^- \to \Lambda\bar{\Lambda}$ at 12 energy intervals where the results show a behavior that favors a non-zero value at threshold. This is contrary to expectations, given the fact that the Coulomb factor does not play any role according to Equation (1) for the neutral baryon pairs. However, uncertainties are large due to the limited statistics and finite energy resolution, thus a vanishing cross section at threshold cannot be excluded. The BESIII experiment has measured the Born cross section of $e^+e^- \to \Lambda\bar{\Lambda}$ at $\sqrt{s} = 2.2324$ GeV, to be $305 \pm 45^{+66}_{-36}$ pb from a weight-average value of two decay final states as introduced in Section 2.5. The result is larger than the theory expectation for neutral baryon pairs, which confirms the non-vanishing cross section speculated from BaBar's results. A fit based on the expectation that the cross section should be proportional to the phase space factor times a pQCD driven energy power [26],

$$\sigma^B = \frac{c_0\beta}{(\sqrt{s} - c_1)^{10}} \tag{4}$$

is presented in Figure 3a, where c_0 and c_1 are two float parameters. The experimental results can be well described with the pQCD-motivated prediction except for the energy point of $\sqrt{s} = 2.2324$ GeV. Therefore, more theoretical interpretations are responsible for the threshold enhancement effect in the cross section of $e^+e^- \to \Lambda\bar{\Lambda}$ and will be discussed in Section 4.

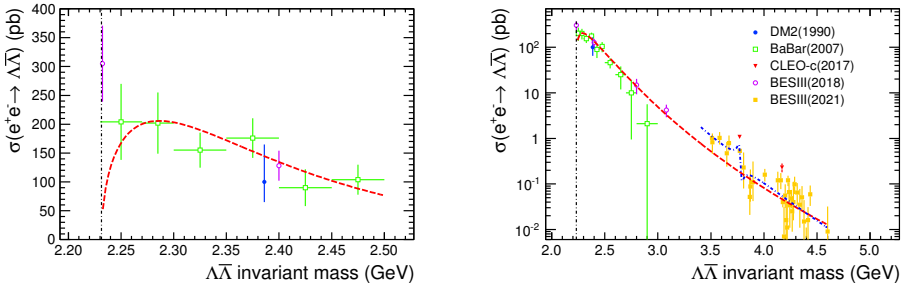

(**a**) (**b**)

Figure 3. (**a**) The Born cross section of $e^+e^- \to \Lambda\bar{\Lambda}$ for $\Lambda\bar{\Lambda}$ masses from 2.0 to 2.5 GeV. The solid circle in blue is from DM2, the open square in green is from BaBar and the open circle in violet is from BESIII. Dashed line indicates fit results according to Equation (4). (**b**) Results of cross section for $e^+e^- \to \Lambda\bar{\Lambda}$ in a wide c.m. energy region from threshold to 4.6 GeV. The dash-dotted line in blue is the fit function introduced in Ref. [14].

The experiments CLEO-c [12] and BESIII [14] have performed the measurement of $e^+e^- \to \Lambda\bar{\Lambda}$ at higher c.m. energies $\sqrt{s} \geq 3.77$ GeV. At BESIII, the Born cross section of the process $e^+e^- \to \Lambda\bar{\Lambda}$ is measured at 33 c.m. energies from $\sqrt{s} = 3.51$ to 4.60 GeV using a data set corresponding to a total integrated luminosity of 20.0 fb^{-1}. The Born cross section decreases from 1 pb to 0.01 pb as predicted by the pQCD. However, when extrapolating the pQCD-motivated function to the high energies, obvious discrepancy is observed between theoretical prediction and experimental results. In Ref. [14], a fit with coherent sum of the phase space and a Breit-Wigner function is performed in the energy region of 3.51 to 4.6 GeV, and the resonance contribution from $\psi(3770) \to \Lambda\bar{\Lambda}$ is observed with a significance over 3σ. The two fit results as well as the experimental results are illustrated in Figure 3b. CLEO-c has measured the cross sections of $e^+e^- \to \Lambda\bar{\Lambda}$ at $\sqrt{s} = 3.77$ and 4.16 GeV and the results are shown in Figure 3b. However, there is tension for cross section of $e^+e^- \to \Lambda\bar{\Lambda}$ at $\sqrt{s} = 3.77$ GeV between CLEO-c and BESIII results, which is $1.08 \pm 0.09 \pm 0.04$ pb for CLEO-c and $0.53 \pm 0.03 \pm 0.02$ pb for BESIII. Further investigation concerning the difference should be examined.

4. Theoretical Discussions

The unexpected features of $\Lambda\bar{\Lambda}$ production cross section from e^+e^- annihilation near threshold have driven a wide theoretical studies, including the final-states interactions (FSI) [30] and scenarios that invoke bound states or unobserved meson resonances [31–33], and interpretations that an attractive Coulomb interaction happens at the constituent quark level [34,35].

In the reaction of $\bar{p}p \to \bar{\Lambda}\Lambda$, various models have been studied in terms of the constituent quark model or by the exchange of strange mesons. Among them, the Jülich meson-exchange model has achieved a good description of all PS185 data [36] by taking into account the effects of initial or final state interactions rigorously. With the similar $\Lambda\bar{\Lambda}$ potential models, the cross section of $e^+e^- \to \Lambda\bar{\Lambda}$ from BaBar results can be well reproduced [30]. However, the non-zero cross section at $\sqrt{s} = 2.2324$ GeV of BESIII results cannot be described by the $\Lambda\bar{\Lambda}$ FSI, as the theory predicts a pure S-wave very close to threshold.

The threshold enhancement of BESIII result is then investigated by considering possible resonances exist. In Ref. [31], two resonances, $\phi(2170)$ and another near 2.34 GeV, are used to explain the close-to-threshold enhancement and the energy dependency above the threshold, respectively. In Ref. [32], the mass spectrum of the strangeonium system is investigated with the double baryon decay widths from the excited vector strangeonium state ϕ^*. It is found that the partial decay width of the $\Lambda\bar{\Lambda}$ mode can reach up to 5.84 MeV for $\phi(3S)$, while the partial $\Lambda\bar{\Lambda}$ decay width of the states $\phi(2D)$ is about $\mathcal{O}(10^{-3})$ keV. Thus, the $\Lambda\bar{\Lambda}$ decay width ratio between the states $\phi(3^3S_1)$ and $\phi(2^3D_1)$ is $\mathcal{O}(10^6)$. It is concluded from Ref. [32] that, if the threshold enhancement reported by the BESIII experiment in the process $e^+e^- \to \Lambda\bar{\Lambda}$ does arise from an unobserved strangeonium meson, the resonance is most likely to be the strangeonium state $\phi(3S)$. In Ref. [33], the $e^+e^- \to \Lambda\bar{\Lambda}$ reaction near threshold and the electromagnetic form factors of the Λ hyperon within the modified vector meson dominance model (VMD) are studied. In addition to these contributions from the ground ω and ϕ mesons, a narrow vector meson $X(2232)$ with a mass around the mass threshold of $\Lambda\bar{\Lambda}$ and a width of about a few MeV is introduced. Thus the threshold enhancement of the total cross sections of the $e^+e^- \to \Lambda\bar{\Lambda}$ reaction at $\sqrt{s} = 2.2324$ GeV can be well reproduced. This narrow state could be the ϕ excitation as predicted in Ref. [32], or a $\Lambda\bar{\Lambda}$ quasi-bound state with quantum numbers $J^{PC} = 1^-$.

It has also been pointed out that the Coulomb correction factor C in Equation (1), which takes the pointlike fermion pair production account, need to be further corrected since the baryons are non-pointlike particles in the energy scale near threshold [34,35]. Therefore, the threshold enhancement in the cross section of $e^+e^- \to \Lambda\bar{\Lambda}$ might be due to the strong interaction at the quark level. After considering the repulsive Coulomb interaction at the quark level, the cross section of $e^+e^- \to \Lambda\bar{\Lambda}$ at threshold can be expressed as

$$\sigma^B = \frac{\pi^2\alpha^3}{2m_\Lambda^2}(Q_u^2 + Q_d^2 + Q_s^2) \cdot |G|^2 \tag{5}$$

where $|G|$ is the effective form factors of Λ at threshold, and Q_q $(q = u, d, s)$ is the charge of valence quark. By analogy with the proton case, one can expect the cross section of $e^+e^- \to \Lambda\bar{\Lambda}$ at threshold will be in the range of around 0.4 nb, which is comparable to the experimental results near threshold.

5. Conclusions and Prospect

Various experiments have measured the production of the $\Lambda\bar{\Lambda}$ final states. Threshold effect is observed in e^+e^- experiments which indicates a complex mechanism in the $\Lambda\bar{\Lambda}$ production. However, the statistics is still limited that more precise measurements are desired. Besides, there are disagreements observed among various experimental measurements in both the $\bar{p}p$ and e^+e^- experiments. Therefore, further investigation of the $\Lambda\bar{\Lambda}$ production in a wide c.m. energies is necessary. In future, the PANDA experiment at the

HESR storage ring at FAIR [37] will measure the $\bar{p}p \to \bar{\Lambda}\Lambda$ reaction over a wide energy region using data samples orders of magnitude larger than all experiments before. This will allow for precision studies of the cross section production, polarization, spin-correlation of Λ. Moreover, BelleII [38] and BESIII [39] experiments will collect huge integrated luminosities of e^+e^- collidering data, e.g., 50 ab^{-1} at c.m. energy around 10 GeV and 20 fb^{-1} at $\sqrt{s} = 3.773$ GeV, respectively. Cross sections of $e^+e^- \to \Lambda\bar{\Lambda}$ over a wide $\Lambda\bar{\Lambda}$ spectrum with improved precision will be achieved with the ISR approach using $e^+e^- \to \Lambda\bar{\Lambda}\gamma_{ISR}$, which allows to examine any possible intermediate states. It should be worth to note that, the importance of the future experiments is not just the improvement of the statistics, but also the improvement of the experimental method as well as the systematic uncertainties, considering the controversy existing in current experiments.

Author Contributions: Conceptualization, X.Z., L.Y., R.B.F. and G.H.; methodology, X.Z., L.Y., R.B.F. and G.H.; validation, X.Z., L.Y., R.B.F. and G.H.; formal analysis, X.Z., L.Y., R.B.F. and G.H.; investigation, X.Z., L.Y., R.B.F. and G.H.; writing—original draft preparation, X.Z., L.Y., R.B.F. and G.H.; writing—review and editing, X.Z., L.Y., R.B.F. and G.H. All authors have read and agreed to the published version of the manuscript.

Funding: The work is supported in part by National Natural Science Foundation of China (NSFC) under Contracts Nos. 12035013, 12061131003, 11335008, 11911530140; National Key Research and Development Program of China 2020YFA0406403; Joint Large-Scale Scientific Facility Funds of the NSFC and CAS under Contracts No. U1832103; This research is sponsored by Shanghai Pujiang Program(20PJ1401700); USTC Research Funds of the Double First-Class Initiative YD2030002005 and the Fundamental Research Funds for the Central Universities.

Institutional Review Board Statement: Not applicable.

Informed Consent Statement: Not applicable.

Data Availability Statement: The original data are made publicly avaliable by the referred collaborations.

Acknowledgments: The authors gratefully thank the editors of the special issue of the journal, Monica Bertani, Simone Pacetti and Alessio Mangoni for the organization and helps. The auhors would like to thank Paul Larin for the careful reading and valuable suggestions for this paper.

Conflicts of Interest: The authors declare no conflict of interest.

References

1. Hopper, V.D.; Biswas, S. Evidence Concerning the Existence of the New Unstable Elementary Neutral Particle. *Phys. Rev.* **1950**, *80*, 1099. [CrossRef]
2. Danysz, M.; Pniewski, J. Delayed disintegration of a heavy nuclear fragment. *Philos. Mag.* **1953**, *44*, 350. [CrossRef]
3. Burkardt, M.; Dillig, M. $\bar{p}p \to \bar{\Lambda}\Lambda$ Reaction in the One Gluon Exchange and the Triplet *P* Wave Models. *Phys. Rev. C* **1988**, *37*, 1362–1364. [CrossRef] [PubMed]
4. Particle Data Group. The Review of Particle Physics. *Prog. Theor. Exp. Phys.* **2020**, *2020*, 1–2093.
5. Cabibbo, N.; Gatto, R. Electron Positron Colliding Beam Experiments. *Phys. Rev.* **1961**, *124*, 1577–1595. [CrossRef]
6. Schwinger, J. *Particle, Sources, and Field*; Perseus Books Publishing: New York, NY, USA, 1998; Volume 3.
7. Arbuzov, A.B.; Kopylova, T.V. On relativization of the Sommerfeld-Gamow-Sakharov factor. *J. High Energy Phys.* **2012**, *1204*, 9. [CrossRef]
8. Barnes, P.D.; Besold, R.; Birien, P.; Bonner, B.E.; Breunlich, W.H.; Diebold, G.; Dutty, W.; Eisenstein, R.A.; Ericsson, G.; Eyrich, W.; et al. Threshold Measurement of the Reaction $\bar{p}p \to \Lambda\bar{\Lambda}$ at LEAR. *Phys. Lett. B* **1989**, *229*, 432–438. [CrossRef]
9. Barnes, P.D.; Birien, P.; Breunlich, W.H.; Dutty, W.; Eisentein, R.A.; Ericsson, G.; Eyrich, W.; Fischer, H.; Frankenberg, R.V.; Franklin, G.; et al. Study of the reaction $\bar{p}p \to \bar{\Lambda}\Lambda$ below 6-MeV excess energy. *Phys. Lett. B* **1994**, *331*, 203–210. [CrossRef]
10. Barnes, P.D.; Franklin, G.; McCrady, R.; Merrill, F.; Meyer, C.; Quinn, B.; Schumacher, R.A.; Zeps, V.; Hamann, N.; Eyrich, W.; et al. High statistics measurements of the $\bar{p}p \to \Lambda\bar{\Lambda}$ and $\bar{p}p \to \Lambda\bar{\Sigma} + c.c$ reactions at threshold. *Phys. Rev. C* **2000**, *62*, 055203.
11. Bisello, D.; Busetto, G.; Castro, A.; Nigro, M.; Pescara, L.; Posocco, M.; Sartori, P.; Stanco, L.; Antonelli, A.; Biagini, M.E.; et al. DM2 Collaboration. Baryon pair production in e^+e^- annihilation at $\sqrt{s} = 2.4$ GeV. *Z. Phys. C* **1990**, *48*, 23–28.
12. Dobbs, S.; Seth, K.K.; Tomaradze, A.; Xiao, T.; Bonvicini, G. Hyperon Form Factors & Diquark Correlations. *Phys. Rev. D* **2017**, *96*, 092004.
13. Ablikim, M.; Achasov, M.N.; Ahmed, S.; Ai, X.C.; Albayrak, O.; Albrecht, M.; Ambrose, D.J.; Amoroso, A.; An F.F.; An Q.; et al. Observation of a cross-section enhancement near mass threshold in $e^+e^- \to \Lambda\bar{\Lambda}$. *Phys. Rev. D* **2018**, *97*, 032013. [CrossRef]

14. Ablikim, M.; Achasov, M.N.; Adlarson, P.; Ahmed, S.; Albrecht, M.; Aliberti, R.; Amoroso, A.; An M.R.; An Q.; Bai, X.H.; et al. Measurement of the Cross Section for $e^+e^- \to \Lambda\bar{\Lambda}$ and Observation of the Decay $\psi(3770) \to \Lambda\bar{\Lambda}$. *Phys. Rev. D* **2021**, *104*, L091104. [CrossRef]
15. Aubert, B.; Bona, M.; Boutigny, D.; Karyotakis, Y.; Lees, J.P.; Poireau, V.; Prudent, X.; Tisser, V.; Zghiche, A.; Tico, J.; et al. BaBar Collaboration. Study of $e^+e^- \to \Lambda\bar{\Lambda}$, $\Lambda\bar{\Sigma}^0$, $\Sigma^0\bar{\Sigma}^0$ using initial state radiation with BABAR. *Phys. Rev. D* **2007**, *76*, 092006. [CrossRef]
16. Budker, G.I.; Skrinsky, A.N. The electron Cooling and New Possibilities in Elementary Particle Physics. *Sov. Phys. Uspekhi* **1978**, *21*, 277–298. [CrossRef]
17. Augustin, J.E.; Bussetto, G.; Capon, G.; Cosme, G.; Dudelzak, B.; Eschstruth, P.; Fulda, F.; Grelaud, B.; Grosdidier, G.; Jean-Marie, B.; et al. Dm2: A Magnetic Detector for the Orsay Storage Ring DCI. *Phys. Scr.* **1981**, *23*, 623–633. [CrossRef]
18. Aubert, B.; Bazan, A.; Boucham, A.; Boutigny, D.; De Bonis, I.; Favier, J.; Gaillard, J.-M.; Jeremie, A.; Karyotakis, Y.; Le Flour, T.; et al. BaBar Collaboration. The BaBar detector. *Nucl. Instrum. Meth. A* **2002**, *479*, 1–116. [CrossRef]
19. Dobbs, S.; Metreveli, Z.; Seth, K.K.; Tomaradze, A.; Ecklund, K.M.; Love, W.; Savinov, V.; Lopez, A.; Mehrabyan, S.; Mendez, H.; et al. CLEO Collaboration. Measurement of absolute hadronic branching fractions of D mesons and $e^+e^- \to D\bar{D}$ cross-sections at the $\psi(3770)$. *Phys. Rev. D* **2007**, *76*, 112001. [CrossRef]
20. Ablikim, M.; An, Z.H.; Bai, J.Z.; Berger, N.; Bian, J.M.; Cai, X.; Cao, G.F.; Cao, X.X.; Chang, J.F.; Chen, C.; et al. Design and Construction of the BESIII Detector. *Nucl. Instrum. Meth. A* **2010**, *614*, 345–399. [CrossRef]
21. Ablikim, M.; Achasov, M.N.; Saher, A.; Albrecht, M.; Antonio, A.; An, F.F.; An Q.; Bai, J.Z.; Bai, Y.; Bakina, O.; et al. Study of J/ψ and $\psi(3686)$ decay to $\Lambda\bar{\Lambda}$ and $\Sigma^0\bar{\Sigma}^0$ final states. *Phys. Rev. D* **2017**, *95*, 052003. [CrossRef]
22. Besiii Collaboration. Polarization and Entanglement in Baryon-Antibaryon Pair Production in Electron-Positron Annihilation. *Nat. Phys.* **2019**, *15*, 631–634. [CrossRef]
23. Ablikim, M.; Achasov, M.N.; Adlarson, P.; Ahmed, S.; Albrecht, M.; Alekseev, M.; Amoroso, A.; An F.F.; An Q.; Bai, Y.; et al. Complete Measurement of the Λ Electromagnetic Form Factors. *Phys. Rev. Lett.* **2019**, *123*, 122003. [CrossRef] [PubMed]
24. Ablikim, M.; Achasov, M.N.; Adlarson, P.; Ahmed, S.; Albrecht, M.; Aliberti, R.; Amoroso, A.; An M.R.; An Q.; Bai, X.H.; et al. Measurement of Λ baryon polarization in $e^+e^- \to \Lambda\bar{\Lambda}$ at $\sqrt{s} = 3.773$ GeV. *arXiv* **2021**, arXiv:2111.11742.
25. Huang, G.; Ferroli, R.B. Probing the internal structure of baryons. *Natl. Sci. Rev.* **2021**, *8*, nwab187. [CrossRef]
26. Pacetti, S.; Ferroli, R.B.; Tomasi-Gustafsson, E. Proton electromagnetic form factors: Basic notions, present achievements and future perspectives. *Phys. Rept.* **2015**, *550–551*, 1–103. [CrossRef]
27. Carbonell, J.; Protasov, K.V.; Dalkarov, O.D. On a possible near threshold Lambda Anti-lambda state. *Phys. Lett. B* **1993**, *306*, 407–410. [CrossRef]
28. Bugg, D.V. Partial wave analysis of $\bar{p}p \to \bar{\Lambda}\Lambda$. *Eur. Phys. J. C* **2004**, *36*, 161–168. [CrossRef]
29. Klempt, E.; Bradamante, F.; Martin, A.; Richard, J.M. Antinucleon nucleon interaction at low energy: Scattering and protonium. *Phys. Rep.* **2002**, *368*, 119–316. [CrossRef]
30. Haidenbauer, J.; Meißner, U.G. The electromagnetic form factors of the Λ in the timelike region. *Phys. Lett. B* **2016**, *761*, 456–461. [CrossRef]
31. Cao, X.; Dai, J.P.; Xie, Y.P. Vector mesons and electromagnetic form factor of the Λ hyperon. *Phys. Rev. D* **2018**, *98*, 094006. [CrossRef]
32. Xiao, L.Y.; Weng, X.Z.; Zhong, X.H.; Zhu, S.L. A possible explanation of the threshold enhancement in the process $e^+e^- \to \Lambda\bar{\Lambda}$. *Chin. Phys. C* **2019**, *43*, 113105. [CrossRef]
33. Li, Z.Y.; Dai, A.X.; Xie, J.J. Electromagnetic form factors of Λ hyperon in the vector meson dominance model and the near-threshold enhancement of the $e^+e^- \to \Lambda\bar{\Lambda}$ reaction. *arXiv* **2019**, arXiv:2107.10499.
34. Baldini, R.; Pacetti, S.; Zallo, A.; Zichichi, A. Unexpected features of $e^+e^- \to p\bar{p}$ and $e^+e^- \to \Lambda\bar{\Lambda}$ cross sections near threshold. *Eur. Phys. J. A* **2009**, *39*, 315–321. [CrossRef]
35. Brodsky, S.J.; Hoang, A.H.; Kuhn, J.H.; Teubner, T. Angular distributions of massive quarks and leptons close to threshold. *Phys. Lett. B* **1995**, *359*, 355–361. [CrossRef]
36. Haidenbauer, J.; Holinde, K.; Mull, V.; Speth, J. Meson exchange and quark - gluon transitions in the anti-p p $\to$ anti-Lambda Lambda process. *Phys. Rev. C* **1992**, *46*, 2158–2171. [CrossRef]
37. Lutz, M.F.M. Physics Performance Report for PANDA: Strong Interaction Studies with Antiprotons. *arXiv* **2009**, arXiv:0903.3905.
38. Kou, E. The Belle II Physics Book. *PTEP* **2019**, *2019*, 123C01. [CrossRef]
39. Ablikim, M.; Achasov, M.N.; Adlarson, P.; Ahmed, S.; Albrecht, M.; Alekseev, M.; Amoroso, A.; An F.F.; An Q.; Bai, Y.; et al. Future Physics Programme of BESIII. *Chin. Phys. C* **2020**, *44*, 040001. [CrossRef]